Int. J. Appl. Math. Comput. Sci., 2023, Vol. 33, No. 2, 219–228
DOI: 10.34768/amcs-2023-0017

AN EFFICIENT FAULT TOLERANT CONTROL SCHEME FOR EULER–LAGRANGE SYSTEMS

IVON E. LEAL-LEAL [a], EFRAIN ALCORTA-GARCIA [a,*]

[a]Faculty of Electrical and Mechanical Engineering
Autonomous University of Nuevo Leon
Av. Universidad S/N, San Nicolas de los Garza, N.L., 66455, Mexico
e-mail: {ivon.lealll,efrain.alcortagr}@uanl.edu.mx

Every closed-loop system holds a level of fault tolerance, which could be increased by using a fault tolerant control (FTC) scheme. In this paper, an efficient FTC scheme for a class of nonlinear systems (Euler–Lagrange ones) is proposed, which guarantees high performance and stability in a faulty system. This scheme was designed on the basis of a cascade control structure in which the inner loop is the closed-loop system and the external loop is the FTC, a generalized proportional integral (GPI) observer-based controller, which manages the fault tolerance level increment. An important issue of the proposed scheme is that the GPI observer-based controller jointly estimates disturbances and faults, providing information about the state of health of the system, and then compensates their effect. The scheme is efficient because only the inertia matrix is required for the controller design, it is able to preserve the nominal control law unchanged and can operate properly without explicit information about system faults (fault diagnostic module). Simulation results, on a pendulum model, show the effectiveness of the proposed scheme for tracking control.

Keywords: cascade structure, Euler–Lagrange systems, FTC scheme, GPI observer-based controller.

1. Introduction

With the emergence of increasingly complex industrial processes, due to the large number of variables and nonlinearities present, there is a greater probability of undesirable system operation. Consequently, the growing demand for safety and reliability in industrial processes requires of the control approaches to be efficient, i.e., easy to design and implement, and to can cope with faults on their sensors, actuators and components. Note that the word ‘efficient’ is being used in a colloquial sense. It is important to stress that a fault is understood as a parameter change beyond the designed tolerance limits.

In the control literature, several fault tolerant control (FTC) approaches have been proposed, as can be seen in the survey papers by Yu and Jiang (2015) or Gao *et al*. (2015) and the references therein. However, most of these FTC approaches are for linear systems or for a class of nonlinear systems, and require modifications of the close-loop system in order to achieve fault tolerance. Furthermore, most of them need an exact mathematical model, built from the dynamics involved in the process. Thus, the FTC problem has begun to attract increasing attention in a wider range of industrial processes, due to increased safety and reliability demands. Many research papers have dealt with the design of FTC for a variety of complex applications (e.g., Hamayun *et al*., 2015; Li *et al*., 2018; Salazar *et al*., 2020).

In some industrial processes it is difficult or impossible to modify the closed-loop system to add an FTC one. For example, in flight control systems it is more efficient to use an FTC design independently of the existing nominal flight control, i.e., the control law is reconfigured by adding an external FTC loop to compensate the faults. This is an interesting aspect of the design scheme, because the overall concept ensures specified nominal flight performance in fault-free situations (e.g., Cieslak *et al*., 2008; 2010). Therefore, having an FTC scheme that keeps the closed-loop system unchanged would be an important advantage. Also, in the work of Rodriguez-Alfaro *et al*. (2013) a cascade control structure for fault tolerance is proposed. This structure uses an additional control loop and a new

*Corresponding author

controller. As a result, the closed-loop system and therefore the nominal control law remain unaltered after reconfiguration. However, the approach requires knowledge of the complete mathematical model and of the nominal control law for the design.

The design of efficient controllers, with the least possible amount of information about the system, is a challenging problem. GPI observer-based control is a robust control designed in the context of active disturbance rejection control (ADRC) (Sira-Ramírez *et al.*, 2018), in which simplified models of systems are used and no modeled dynamics, internal or external disturbances of the system are estimated by a GPI observer, i.e., the unknown variables are algebraically observable (e.g., Flores-Flores and Martinez-Guerra, 2019).

Generalized PI observers are linear observers characterized by an internal, self-updating, time-polynomial model of unknown, uniformly bounded, disturbances. The main application of the GPI observer is when it is used in line with its controller (generalized PI observer-based control), where the unknown variables are rejected jointly and approximately. Recently, GPI observer-based control has been utilized to improve tracking performance of robot manipulators (Gutiérrez Giles *et al.*, 2016). This controller has the advantage of requiring little amount of information about the mathematical model of the system—only the inertial matrix. However, a robust controller designed for a closed-loop system generally works fine for the nominal system, but fails for a faulty system. Therefore, it is necessary to develop and incorporate, increasingly, FTC approaches which can be applied to a wide range of nonlinear systems to ensure effectiveness and improve the system's reliability.

In the present paper we propose an efficient FTC scheme to increase fault tolerance, which seeks to achieve performance and stability typical for a nominal system in a faulty system, for a class of non-linear systems called Euler–Lagrange (EL) ones (Van der Schaft, 2000). This idea will be implemented using the theory of GPI observer-based control, which has very interesting robustness properties, where we want to take advantage of the approximation of the disturbances that the GPI observer allows us to have in order to also approximate faults and then compensate their effect in the control stage. The proposed scheme was designed on the basis of a cascade control structure, in which a new control loop is proposed, feeding back the actual output and making the difference with the nominal output. The "plant" for this new loop corresponds to the original closed-loop system. As a result, the proposed approach was able to preserve the inner loop formed by the closed-loop system unchanged. The scheme utilizes an external GPI observer-based control as FTC, which manages the fault tolerance level increment.

The paper is organized as follows. After Introduction, the preliminaries related to FTC, the cascade control structure and GPI observer-based control are reviewed in Section 2. The proposed approach is presented and justified in Section 3. A simulation example with a pendulum model (described by Sira-Ramírez *et al.*, 2010) is shown in Section 4. Finally, the conclusions are presented in Section 5.

2. Preliminaries

2.1. GPI observer based control. The so-called GPI observer-based control has been established as an efficient control technique which is robust to classical disturbances (Sira-Ramírez *et al.*, 2010). The GPI observer-based control proposed by Gutiérrez Giles *et al.* (2016) considers E–L systems given by

$$\mathbf{H}(\mathbf{q})\ddot{\mathbf{q}} + \mathbf{C}(\mathbf{q},\dot{\mathbf{q}})\dot{\mathbf{q}} + \mathbf{g}(\mathbf{q}) = \boldsymbol{\tau}, \tag{1}$$

where $\mathbf{q} \in \mathbb{R}^n$ is the vector of the generalized coordinates, $\mathbf{H}(\mathbf{q}) \in \mathbb{R}^{n\times n}$ is the generalized inertia matrix, $\mathbf{C}(\mathbf{q},\dot{\mathbf{q}})\dot{\mathbf{q}} \in \mathbb{R}^n$ is the vector of Coriolis and centrifugal forces, $\mathbf{g}(\mathbf{q}) \in \mathbb{R}^n$ are the forces generated by potential fields such as the gravitational field, and $\boldsymbol{\tau} \in \mathbb{R}^n$ is the vector of control inputs.

The basic design of a GPI observer can be carried out with only the knowledge of the position vector, $\mathbf{q}$, and the inertia matrix, $\mathbf{H}(\mathbf{q})$. The goal of this design is to compute estimates for the uncertain terms and for the error dynamics, denoted by $\boldsymbol{\xi}$ and $\dot{\mathbf{e}}$, respectively. Then $\boldsymbol{\xi} \in \mathbb{R}^n$ represents the unknown perturbation vector and can be expressed as

$$\boldsymbol{\xi}(t) = \sum_{i=0}^{p-1} \mathbf{a}_i t^i + \mathbf{r}(t), \tag{2}$$

with each $\mathbf{a}_i$ being an n-vector of constant coefficients (and at least the first p derivatives of the residual term $\mathbf{r}(t)$ exist). The GPI observer-based control is based on integral re-constructors and is given by

$$\begin{aligned}
\boldsymbol{\tau}(t) &= \mathbf{H}(\mathbf{q}) \left[-2\boldsymbol{\zeta}\boldsymbol{\omega}_{\mathrm{n}}\hat{\mathbf{e}}(\mathbf{t}) - \boldsymbol{\omega}_{\mathrm{n}}^{\mathbf{2}}\mathbf{e}(t) - \hat{\boldsymbol{\xi}}(t)\right], \qquad (3)\\
\dot{\hat{\mathbf{e}}}_1(t) &= \hat{\mathbf{e}}_2(t) + \lambda_{p+1}\tilde{\mathbf{e}}(t),\\
\dot{\hat{\mathbf{e}}}_2(t) &= \mathbf{H}^{-1}(\mathbf{q})\boldsymbol{\tau}(t) + \hat{\boldsymbol{\xi}}_1(t) + \lambda_p\tilde{\mathbf{e}}(t),\\
\dot{\hat{\boldsymbol{\xi}}}_{\mathbf{1}}(t) &= \hat{\boldsymbol{\xi}}_2(t) + \lambda_{p-1}\tilde{\mathbf{e}}(t),\\
&\vdots\\
\dot{\hat{\boldsymbol{\xi}}}_{p-1}(t) &= \hat{\boldsymbol{\xi}}_p(t) + \lambda_1\tilde{\mathbf{e}}(t),\\
\dot{\hat{\boldsymbol{\xi}}}_{\mathbf{p}}(t) &= \lambda_0\tilde{\mathbf{e}}(t),
\end{aligned}$$

where $\hat{\boldsymbol{\xi}}(t) = \hat{\boldsymbol{\xi}}_1(t)$, $\hat{\mathbf{e}}(t) = \hat{\mathbf{e}}_2(t)$. The GPI control globally asymptotically drives the error vector, $\tilde{\mathbf{e}}(t) =$

$\mathbf{e}(t) - \hat{\mathbf{e}}_1(t)$, and its time derivative, $\dot{\tilde{\mathbf{e}}}(t) = \dot{\mathbf{e}}(t) - \hat{\mathbf{e}}_2(t)$, to an arbitrary small neighborhood of the origin of the reconstruction error of the tracking error vector space, $(\tilde{\mathbf{e}}, \dot{\tilde{\mathbf{e}}})$. Therefore the diagonal, constant matrices $\{\boldsymbol{\lambda}_0, \boldsymbol{\lambda}_1, \cdots, \boldsymbol{\lambda}_{p+1}\} \in \mathbb{R}^{n\times n}$ are chosen in such a way that all the non-zero components of the $n \times n$ complex valued diagonal matrix, $\mathbf{p}_o(s)$, defined as

$$\mathbf{p}_o(s) = s^{p+2}\mathbf{I} + \boldsymbol{\lambda}_{p+1}s^{p+1} + \cdots + \boldsymbol{\lambda}_1 s + \boldsymbol{\lambda}_0, \quad (4)$$

are Hurwitz polynomials of degree $p+2$ with roots located sufficiently far into the left half of the complex plane.

In the controller design $\mathbf{I}_n \in \mathbb{R}^{n\times n}$ denote the identity matrix and $\boldsymbol{\zeta} \in \mathbb{R}^{n\times n}$ and $\boldsymbol{\omega}_\mathrm{n} \in \mathbb{R}^{n\times n}$ are chosen in such a way that all the elements of the diagonal matrix of the polynomial of Eqn. (5) are second degree Hurwitz polynomials

$$\mathbf{p}_c(s) = s^2\mathbf{I}_n + 2\boldsymbol{\zeta}\boldsymbol{\omega}_n s + \boldsymbol{\omega}_n^2. \quad (5)$$

2.2. Fault tolerant control (FTC). The objective of FTC is to minimize the degradation in performance in the closed-loop system when a fault occurs. Moreover, a reliable FTC scheme maintains the relation between safety and fault tolerance. The safety system and the FTC work in separate regions and satisfy complementary aims, as can be seen in Fig. 1 (taken from Blanke *et al.* (2016)), where the system performance is described. In the region of required performance, the system satisfies its function, and it is the region where the system should remain during its time operation. Note that, because of robustness properties of the closed-loop system, almost every system holds a level of tolerance with respect to a given fault. Consequently, the nominal control may even hold the system in the region of required performance if small faults occurs, although this is not its primary goal. Alternatively, the FTC should be able to initiate recovery actions that prevent further degradation of the performance towards unacceptable or dangerous regions, and it should move the system back into the region of required performance.

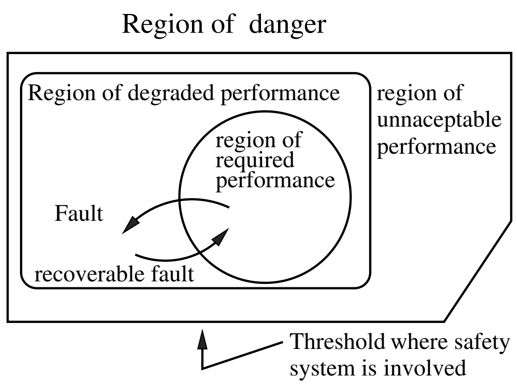

Fig. 1. Regions of required and degraded performance.

Consider a nonlinear system given by

$$\dot{\mathbf{x}}(t) = \boldsymbol{\Gamma}(\mathbf{x}, \mathbf{u}, \mathbf{f}), \quad (6)$$
$$\mathbf{y}(t) = \mathbf{h}(\mathbf{x}, \mathbf{u}, \mathbf{r}), \quad (7)$$

where $\mathbf{x} \in \mathbb{R}^n$ is the state vector, $\mathbf{u} \in \mathbb{R}^m$ is the input vector, $\mathbf{f} \in \mathbb{R}^{n_s}$ is the fault vector. Note that $\mathbf{f}_i$ represents the i-th element of the fault vector $\mathbf{f}$.

In this paper the following definitions are used to give a framework for the results.

Definition 1. (*Fault tolerance*) Given a feedback Euler–Lagrange system and an unknown fault $\mathbf{f}_i(t)$, the system is called fault tolerant to the fault $\mathbf{f}_i(t)$ if in the presence of this fault the closed-loop system remains inside the region of required performance and the following is satisfied:

1. The feedback Euler–Lagrange system remains stable.
2. The system output remains within an admissible tolerance margin with respect to the nominal output.
3. The nominal control law $\boldsymbol{\tau}(\mathbf{t})$ is kept bounded and physically realizable.

The last definition gives us a criterion to know if a system tolerates a specific fault.

Definition 2. (*Recoverable fault*) A fault $\mathbf{f}_i(t)$ which makes the nominal closed-loop system not fault tolerant (the system is in the region of degraded performance), is called "recoverable" if there exists supplementary control effort ($\boldsymbol{\tau}_{\mathrm{FTC}}(t)$) that, when applied in form of a new control loop (see Fig. 2), the resulting closed-loop is fault tolerant with respect to the fault considered (holds the system in the region of required performance).

2.3. Cascade control structure. The cascade control structure (Bolton, 2021) is not new in general but it has not been used intensively in fault tolerance. The cascade control structure initially described by Acosta-Santana *et al.* (2013), formed by an inner loop (closed-loop system) and an external loop (reconfiguration control), is used to increase fault tolerance in control systems (e.g., Rodriguez-Alfaro *et al.*, 2013; Krokavec *et al.*, 2016).

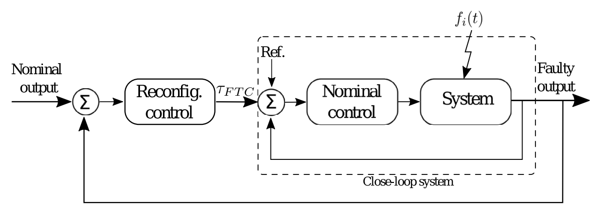

Fig. 2. Structure to get recoverable faults.

Figure 2 shows the cascade control structure for FTC, which uses the nominal system output as reference to be followed when a fault occurs. The estimation error, which is obtained from the difference between the faulty and nominal output, is used as basis for the correction. Then, change a in the nominal system reference in closed loop is carried out and the action of FTC is added to the nominal reference. With this internal reference change, the effect of the fault is eliminated and the faulty system performance is kept very close or equal to the nominal system performance. The cascade structure has the advantage of not modifying the nominal control law. Accordingly, it can be useful in a physical implementation of the fault tolerant scheme.

3. Proposed approach

The state space representation of the system of equations (1) is expressed as

$$\begin{aligned}\dot{\mathbf{x}}_1 &= \mathbf{x}_2,\\ \dot{\mathbf{x}}_2 &= \mathbf{H}^{-1}(x_1,\boldsymbol{\alpha})(\boldsymbol{\tau} - \mathbf{C}(\mathbf{x}_1,\mathbf{x}_2)\mathbf{x}_2 - \mathbf{g}(\mathbf{x}_1)) + \Delta\boldsymbol{d},\end{aligned} \tag{8}$$

where $\mathbf{x} = [\mathbf{q}^T\ \dot{\mathbf{q}}^T] = [\mathbf{x}_1^T\ \mathbf{x}_2^T] \in \mathbb{R}^n$ is the state vector of the system, and $\Delta\boldsymbol{d}$ represents the uncertainties, the unmodeled dynamics and the disturbances in the system.

In this paper additive and multiplicative faults are considered, and it is assumed that the fault occurs at time t_f.

The faults in sensor and actuators are modeled as

$$\begin{aligned}\begin{bmatrix}\dot{\mathbf{x}}_1\\ \dot{\mathbf{x}}_2\end{bmatrix} &= \begin{bmatrix}\mathbf{x}_2\\ \mathbf{x}_2 + \boldsymbol{\Delta} d\end{bmatrix} + \begin{bmatrix}0\\ \mathbf{G}(\mathbf{x})\end{bmatrix}(\boldsymbol{\tau} + \mathbf{f}_a)\\ \mathbf{y} &= \mathbf{C}\mathbf{x} + \mathbf{D}_f\mathbf{f}_s,\end{aligned} \tag{9}$$

where $\mathbf{y} \in \mathbb{R}^n$ is the output vector, $\mathbf{f}_a \in \mathbb{R}^m$ and $\mathbf{f}_s \in \mathbb{R}^q$ are the actuator and sensor faults, respectively, $\mathbf{D}_f \in \mathbb{R}^{n\times q}$ denotes the sensor fault distribution matrix, $\mathbf{F}(\mathbf{x}) = \mathbf{H}^{-1}(\mathbf{x}_1,\boldsymbol{\alpha})(-\mathbf{C}(\mathbf{x}_1,\mathbf{x}_2)\mathbf{x}_2 - \mathbf{g}(x_1))$ and $\mathbf{G}(x) = \mathbf{H}^{-1}(\mathbf{x}_1,\boldsymbol{\alpha})$.

The multiplicative faults are expressed as variations in parameters

$$\boldsymbol{\alpha} = \boldsymbol{\alpha}_0 + \Delta\boldsymbol{\alpha}, \tag{10}$$

where $\boldsymbol{\alpha}$ is the value of any parameter of the system, $\boldsymbol{\alpha}_0$ is the nominal parameter and $\Delta\boldsymbol{\alpha}$ denotes the multiplicative fault.

Moreover, the faults, the uncertainties, the unmodeled dynamics and the disturbances are unknown but bounded, that is, $\|\mathbf{f}_a\| < \bar{\mathbf{f}}_a$, $\|\mathbf{f}_s\| < \bar{\mathbf{f}}_s$, $\|\Delta\boldsymbol{\alpha}\| < \bar{\Delta}\boldsymbol{\alpha}$ and $\|\Delta\boldsymbol{d}\| < \bar{\Delta}\boldsymbol{d}$ for all t.

3.1. Proposed fault tolerant control scheme.

An efficient FTC scheme which estimates and compensates faults in real-time has been developed. The main idea is to incorporate the FTC scheme in the closed-loop system to increase the fault size that can be tolerated. Also, this scheme should preserve the system in the region of required performance to ensure effectiveness and stability under faulty conditions. The proposed scheme has the following desired features:

- Reduced knowledge of the system model is required, i.e., only the inertia matrix.
- It does not require explicit use of the FDI module. In contrast, the proposed scheme makes an estimate of the fault effect and disturbances (an uncertain polynomial, depicted in Fig. 4) regarding the closed-loop system and uses it to compensate their effect.
- It keeps the nominal control law unchanged. This is an important feature in practical applications.
- Only the position measurement of the output is used to design the FTC. Also, nominal output information is required, which can be obtained from a simulation system.

The proposed scheme is based on a cascade control structure, which is connected all the time (not only when a fault occurs), as shown in Fig. 3, where $\mathbf{q}_n$ is the nominal position, $\mathbf{q}$ is the position output measurements, $\mathbf{y}$ is the real output and $\mathbf{y}_d$ is the desired output. The output of the GPI observed-based control represents the correction input to the nominal control, $\boldsymbol{\tau}_{\text{FTC}}(t)$. The external loop error, obtained to reduce the fault effect without changing directly (only in an indirect form) the nominal control, is given by

$$\mathbf{e}(t) = \mathbf{q}(t) - \mathbf{q}_n(t). \tag{11}$$

There are a couple of assumptions related to the proposed solution.

Assumption 1. Only systems with an Euler–Lagrange structure are considered.

Assumption 2. The faults considered are reconfigurable in the sense that there exists a control action to compensate their effect (admissible faults).

The error of the nominal control loop is updated by the correction factor as

$$\mathbf{e}_q(t) = \boldsymbol{\tau}_{\text{FTC}}(t) + \mathbf{y}_d(t) - \mathbf{y}(t). \tag{12}$$

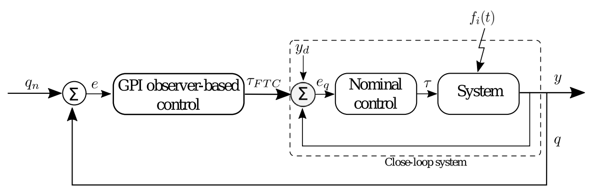

Fig. 3. Cascade control structure for the proposed FTC.

The proposed FTC (GPI observed-based control) is given by

$$
\begin{aligned}
\boldsymbol{\tau}_{\mathrm{FTC}}(t) &= \mathbf{H}(\mathbf{q})(t)\left[-2\boldsymbol{\zeta}\boldsymbol{\omega}_n\hat{\mathbf{e}}(t) - \boldsymbol{\omega}_n^2\mathbf{e}(t) - \hat{\mathbf{z}}(t)\right],\\
\dot{\hat{\mathbf{e}}}_1(t) &= \hat{\mathbf{e}}_2(t) + \lambda_{p+1}\tilde{\mathbf{e}}(t), \qquad (13)\\
\dot{\hat{\mathbf{e}}}_2(t) &= \mathbf{H}^{-1}(\mathbf{q}(\mathbf{t}))\boldsymbol{\tau}(t) + \hat{\mathbf{z}}_1(t) + \lambda_p\tilde{\mathbf{e}}(t),\\
\dot{\hat{\mathbf{z}}}_1(t) &= \hat{\mathbf{z}}_2(t) + \lambda_{p-1}\tilde{\mathbf{e}}(t),\\
&\ \vdots\\
\dot{\hat{\mathbf{z}}}_{p-1}(t) &= \hat{\mathbf{z}}_p(t) + \lambda_1\tilde{\mathbf{e}}(t),\\
\dot{\hat{\mathbf{z}}}_p(t) &= \lambda_0\tilde{\mathbf{e}}(t)
\end{aligned}
$$

where $\hat{\mathbf{z}}(t) = \hat{\mathbf{z}}_1(t)$, $\hat{\dot{\mathbf{e}}}(t) = \hat{\mathbf{e}}_2(t)$, $\tilde{\mathbf{e}}(t) = \mathbf{e}(t) - \hat{\mathbf{e}}_1(t)$.

The outputs of the GPI observer (the error dynamics and the uncertain polynomial, denoted by $\hat{\mathbf{z}}_1$ and $\hat{\dot{\mathbf{e}}}$, respectively) (see Fig. 4), are used by the controller to also compensate the fault effect. The uncertain polynomial,

$$
\mathbf{z}(t) = \sum_{i=0}^{p-1}\mathbf{a}_i t^i + \mathbf{r}(t), \qquad (14)
$$

lumps not only the effects of disturbances and unknown terms, but also the fault terms.

The GPI observed-based control of Eqn. (3) is a robust control (nominal control) which estimates disturbances and uncertain terms; when it used as an external control, it becomes an FTC, and therefore also estimates faults, i.e., the proposed FTC of (13) is robust to disturbances and fault tolerant.

The FDI module is actually not required to activate the FTC (note that the outer control loop processes the difference between the nominal and the actual output, and they play a similar role of a residual); however, it is added because to know the presence of faults is a normal requirement to make decisions about maintenance, as well as to avoid possible faults or possible evolution of a fault not attended. To detect faults, the uncertain polynomial was used. In order to achieve this, a fixed threshold is established (according to the designer's criteria). Once the signal of the uncertain polynomial exceeds the threshold, it will indicate that a fault has occurred (by means of an alarm); see Fig. 5.

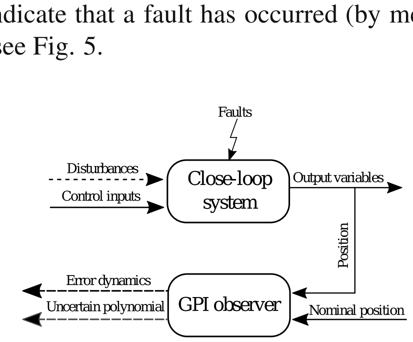

Fig. 4. GPI observer.

Remark 1. The general scheme of the proposed approach does not require the Euler–Lagrange formalism, but in this work advantage is taken of the system model structure, so that the GPI observer-based controller can be formulated with reduced knowledge of the nominal system model (only the inertia matrix $\mathbf{H}(\mathbf{q})$ is required). As pointed out by Ortega *et al.* (2013), because of the facility to manage passivity properties in the Euler–Lagrange structure, regulation problems can be solved by increasing dissipation and redesigning the gravity vector ($\mathbf{g}(\mathbf{q})$).

3.2. Stability analysis in the presence of faults. For the stability analysis, the results of Sira-Ramírez *et al.* (2010) will be evoked. At this point, for the sake of simplicity, the nominal control of the systems is restricted to have an Euler–Lagrange structure, so the nominal feedback system results also in an Euler–Lagrange closed-loop system (see Ortega *et al.*, 2013). In this case, if the faults are absolutely uniformly bounded, then the stability of the whole schema is guaranteed by the results given by Sira-Ramírez *et al.* (2010) (see also Gutiérrez Giles *et al.*, 2016).

The stability proof is exactly taken from the work of Sira-Ramírez *et al.* (2010), and it will be included here for completeness.

Proof. Let the position error vector be defined by $\mathbf{e}_1(t) = \mathbf{q}(t) - \mathbf{q}_n(t)$. Let $\mathbf{e}_2$ be the velocity tracking error, i.e, $\mathbf{e}_2(t) = \dot{\mathbf{q}}(t) - \dot{\mathbf{q}}_n(t)$. The tracking error dynamics, along with the predominantly time polynomial model of perturbation input signal, $\mathbf{z}(t)$, becomes according to Eqn. (14)

$$
\begin{aligned}
\dot{\mathbf{e}}_1(t) &= \mathbf{e}_2(t), \qquad (15)\\
\dot{\mathbf{e}}_2(t) &= \mathbf{H}^{-1}(q(t))\boldsymbol{\tau}_{\mathrm{FTC}}(t) + \mathbf{z}_1(t),\\
\dot{\mathbf{z}}_1(t) &= \mathbf{z}_2(t),\\
&\ \vdots\\
\dot{\mathbf{z}}_{p-1}(t) &= \mathbf{z}_p(t),\\
\dot{\mathbf{z}}_p(t) &= \mathbf{r}^p(t).
\end{aligned}
$$

∎

Let $\tilde{\mathbf{z}}_j = \mathbf{z}_j - \hat{\mathbf{z}}_j$, $j = 1, 2, \dots, p$. The observer reconstruction error vectors $\tilde{\mathbf{e}}_j$ associated with

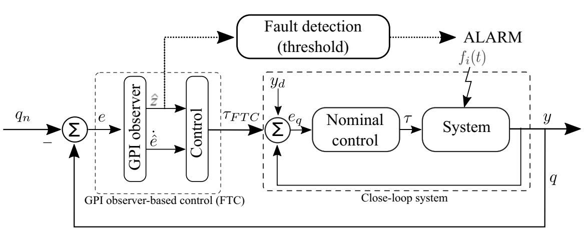

Fig. 5. Proposed FTC scheme.

the generalized position and velocity tracking error, $\mathbf{e}$, $\dot{\mathbf{e}}$, are easily seen to satisfy the following, predominantly linear, perturbed injected dynamics:

$$\begin{aligned} \dot{\tilde{\mathbf{e}}}_1(t) &= \tilde{\mathbf{e}}_2(t) - \lambda_{p+1}\tilde{\mathbf{e}}_1, \\ \dot{\tilde{\mathbf{e}}}_2(t) &= \tilde{\mathbf{z}}_1(t) - \lambda_p\tilde{\mathbf{e}}_1(t), \\ \dot{\tilde{\mathbf{z}}}_1(t) &= \tilde{\mathbf{z}}_2(t) - \lambda_{p-1}\tilde{\mathbf{e}}_1, \\ &\vdots \\ \dot{\tilde{\mathbf{z}}}_{p-1}(t) &= \tilde{\mathbf{z}}_p(t) - \lambda_1\tilde{\mathbf{e}}_1, \\ \dot{\tilde{\mathbf{z}}}_p(t) &= \mathbf{r}^p(t)\lambda_0\tilde{\mathbf{e}}_1. \end{aligned} \tag{16}$$

Eliminating the variables $\tilde{\mathbf{z}}(t)$, we obtain

$$\tilde{\mathbf{e}}^{(p+2)}(t) + \lambda_{p+1}\tilde{\mathbf{e}}^{(p+1)}(t) + \cdots + \lambda_0\tilde{\mathbf{e}} = \mathbf{r}^p(t) = \frac{\mathrm{d}^p}{\mathrm{d}t^p}\mathbf{z}(t). \tag{17}$$

Thanks to (a) our assumptions about the boundedness of the components of the perturbation input vector, $\mathbf{z}(t) \in \mathbb{R}^n$, (b) the boundedness of the continuously updated residual term, $\mathbf{r}(t)$, in the local Taylor polynomial approximation of the signal $\mathbf{z}(t)$, and (c) the well-known results about bounded-input–bounded-output stability theory for linear systems (Kailath, 1980) it is well known that, if the set of matrix coefficients, $\{\boldsymbol{\lambda}_{p+1}, \dots, \boldsymbol{\lambda}_0\}$, of the perturbed linear tracking error dynamics, (16), are chosen so that the polynomials on the complex variable s, in the diagonal of the complex valued diagonal matrix,

$$\mathbf{p}(s) = s^{p+2}\mathbf{I} + \boldsymbol{\lambda}_{p+1}s^{p+1} + \cdots + \boldsymbol{\lambda}_1 s + \boldsymbol{\lambda}_0, \tag{18}$$

are Hurwitz polynomials, with roots located sufficiently far from the imaginary axis in the left half of the complex plane, then the time responses in Eqn. (17) will be asymptotically, exponentially, ultimately bounded by a small disk centered around the origin of the tracking error observer reconstruction error phase space, $\tilde{\mathbf{e}} = \dot{\tilde{\mathbf{e}}} = \ldots = \tilde{\mathbf{e}}^{p+1} = 0$. Moreover, the radius of the ultimate bounding disk, in the phase space of $\tilde{\mathbf{e}}$, is proportional to the inverse of the absolute value of the smallest real part of the roots of the characteristic polynomials found on the diagonal of the matrix (18). As a consequence of the convergence, to an arbitrarily small neighborhood of zero, of the observer reconstruction error for the perturbed tracking error system model, the n-dimensional observer states, $\hat{\mathbf{z}}_1$, become arbitrarily close estimates of the perturbation input functions comprising the n-vector $\mathbf{z}(t)$. Moreover, the consecutive time derivatives of the vector of signals, $\mathbf{z}(t)$, i.e., $\mathbf{z}^j(t)$, $j = 1, 2, \dots$, are also approximately estimated via the corresponding observer vector variables, $\hat{\mathbf{z}}_{j+1}(t)$, $j = 1, 2, \dots$.

4. Application example

The proposed approach is applied to a pendulum model.

4.1. System description. Consider the pendulum system of Fig. 6, consisting of a solid metal bar of length $L = 0.24$ m, mass $M = 0.0883$ kg and extra mass $m = 0.05$ kg. The angular displacement of the motor shaft is θ, the gear ratio is $N = 26$, the moment of inertia is $J = 0.0079$ kg $\cdot$ m^2 and the gravity is $g = 9.8$ m/s^2.

The non-linear pendulum model is

$$\underbrace{\left[J + \frac{L^2}{N^2}\left(\frac{M}{3} + m\right)\right]}_{H_n}\ddot{\theta} + \underbrace{\frac{1}{N}\left(\frac{M}{2} + m\right)gL}_{G_n}\,\mathrm{Sen}(\theta) + B\dot{\theta} + F_c\mathrm{sign}(\dot{\theta}) = \tau, \tag{19}$$

where B is the coefficient of viscous friction and F_c is the Coulomb friction.

Furthermore, consider the pendulum with two types of nominal control. The first is a GPI observer based control, described in Section 2. The second is a proportional derivative control with compensation (PD+), which is a motion control widely used in robots (Kelly and Santibáñez, 2003), whose control law is given by

$$\boldsymbol{\tau} = \mathbf{K}_p\tilde{\mathbf{q}} + \mathbf{K}_v\dot{\tilde{\mathbf{q}}} + \mathbf{H}(\mathbf{q})\ddot{\mathbf{q}}_d + \mathbf{C}(\mathbf{q}, \dot{\mathbf{q}})\dot{\mathbf{q}}_{\mathbf{d}} + \mathbf{g}(\mathbf{q}). \tag{20}$$

Therefore, for the pendulum system, the nominal control (PD+) law is

$$\boldsymbol{\tau} = \mathbf{K}_p\tilde{\mathbf{q}} + \mathbf{K}_v\dot{\tilde{\mathbf{q}}} + \mathbf{H}_n(q)\ddot{\mathbf{q}}_d + \mathbf{G}_n(q)\mathrm{Sen}(\mathbf{q}). \tag{21}$$

Remark 2. In this paper the nominal control law was used to carry out the simulation. But for a physical

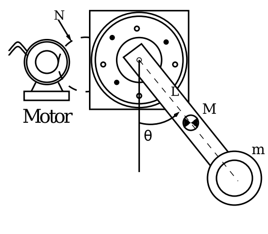

Fig. 6. Pendulum diagram.

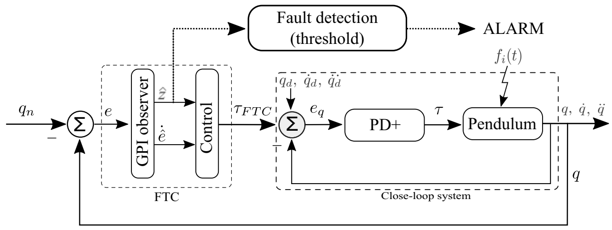

Fig. 7. Semi-active FTC applied to the pendulum (with PD+ control).

implementation it is not required to know the nominal control law.

4.2. System description.

4.3. Simulation. To perform the simulation, the Scilab program was used. The pendulum model with disturbances (19) was implemented.

For the implementation of the controller–observer scheme represented in Eqn. (13), the polynomial order of uncertain or unknown terms was selected as $p = 3$. The controller design parameters were selected as $\zeta = 10$ and $\omega_n = 60$, and the observer design parameters were selected as $\zeta_o = 2$, $\omega_{no} = 10$ and $p_o = 10$, with the following polynomial gains:

$$\begin{aligned} p_o(s) &= (s^2 + 2\zeta_o\omega_{no}s + \omega_{no}^2)^2(s + p_o), \\ \lambda_4 &= p_o + 4\zeta_o\omega_{no}, \\ \lambda_3 &= 2\omega_{no}^2 + 4\zeta_o^2\omega_{no}^2 + 4\zeta_o\omega_{no}p_o, \\ \lambda_2 &= 4\zeta_o\omega_{no}^3 + 2\omega_{no}^2p_o + 4\zeta_o^2\omega_{no}^2p_o, \\ \lambda_1 &= 4\zeta_o\omega_{no}^3p_o + \omega_{no}^4, \\ \lambda_0 &= \omega_{no}^4p_o. \end{aligned}$$

The resulting GPI observer-based FTC is

$$\begin{aligned} \boldsymbol{\tau}_{\mathrm{FTC}}(t) &= \mathbf{H}(q)\left[-2\zeta\omega_n\hat{\mathbf{e}}_2(t) - \omega_n^2\mathbf{e}(t) - \hat{\mathbf{z}}_1(t)\right], \\ \dot{\hat{\mathbf{e}}}_1(t) &= \hat{\mathbf{e}}_2(t) + \lambda_4\tilde{\mathbf{e}}(t), \\ \dot{\hat{\mathbf{e}}}_2(t) &= H^{-1}(q)\boldsymbol{\tau}(t) + \hat{\mathbf{z}}_1(t) + \lambda_3\tilde{\mathbf{e}}(t), \\ \dot{\hat{\mathbf{z}}}_1(t) &= \hat{\mathbf{z}}_2(t) + \lambda_2\tilde{\mathbf{e}}(t), \\ \dot{\hat{\mathbf{z}}}_2(t) &= \hat{\mathbf{z}}_3(t) + \lambda_1\tilde{\mathbf{e}}(t), \\ \dot{\hat{\mathbf{z}}}_3(t) &= \lambda_0\tilde{\mathbf{e}}(t). \end{aligned}$$

The control objective is to track the desired angular displacement of Fig. 8.

4.4. Results and a discussion. Three simulation cases were analyzed in order to demonstrate the fault tolerance increase allowed by the proposed scheme. In Tables 1, 2, and 3 numerical results are shown, where the behavior of the pendulum with two types of nominal control (C_n) and with the proposed FTC (GPI observer-based control) can be observed. The first nominal control is a GPI observer-based control (C_nGPI); this control was selected to compare its behavior when it acts as a nominal control in the inner loop and as an FTC in the external loop. The second nominal control is a PD+ control (C_nPD+); this control was selected because it is widely used in the literature. For the first nominal control and for the proposed FTC the same design parameters presented in Section 4.3 were used. For the second nominal control the design parameters were selected as $K_p = 100$ and $K_v = 50$. Furthermore, the following restrictions were assumed: the maximum torque which can be applied by the actuator is 4.48 N·m ($\|T\| \leq 4.48$), and the physical application of the system does not allow a tracking error greater than $2°$ ($\|e\| \leq 2$). In addition, a threshold between the values ± 1 was considered for fault detection.

Case 1. (*Nominal operating conditions*). In Table 1, it can be seen that, with the nominal controls, the system presents a small error, which can be caused by disturbances, bad control tuning, among others. By adding the FTC loop, or the error decreases because the FTC action is present at all times and not only when the fault occurs.

Case 2. (*Presence of an additive fault f_1*). In Table 2 it can be seen that the FTC can tolerate almost the same fault magnitude as the first nominal control (C_nGPI) , but the error is less than with the nominal control. Also, it can be seen that the FTC can tolerate a higher fault magnitude than the second nominal control (C_n PD+).

Case 3. (*Presence of a multiplicative fault f_2*). In Table 3, it can be seen that the FTC can tolerate a higher fault magnitude than the nominal controls—all this as long as the control action is within the permitted limits.

Then, graphic results are presented for each case, where only, the PD+ control was selected as the nominal control.

In Case 1, for the fault-free system (nominal operation), the tracking errors of Fig. 9 are presented,

where it can be seen that by adding the proposed FTC the error is almost zero.

Table 1. Nominal system with disturbances.

Control	$\|\|T\|\|$ [N·m]	$\|\|e\|\|$ [°]
C_nGPI	0.082	0.912
C_nPD+	0.059	0.031
FTC(C_n PD+)	0.060	0.005

Table 2. System with an actuator fault.

Control	$\|\|T\|\|$ [N·m]	$\|\|e\|\|$ [°]	$\|f_1\|$
C_n GPI	**4.480**	0.911	4.412
C_n PD+	3.496	**2.000**	3.436
FTC(C_n PD+)	**4.480**	0.005	4.419

Table 3. System with a fault due to a mass increase.

Control	$\|\|T\|\|$ [N·m]	$\|\|e\|\|$ [°]	$\|f_2\|$
C_n GPI	0.332	**2.000**	3.339
C_n PD+	3.879	**2.000**	26.220
FTC(C_n PD+)	**4.480**	0.247	49.230

In Case 2, f_1 occurs in the actuator, which delivers 3.4 Nm more than it should and occurs after 10 s ($t_f = 10$).

In Fig. 10, it can be seen that, with the nominal control, we have the maximum permissible error of 2° and, when we add the FTC, the fault effect is compensated.

In Fig. 11, fault detection occurs when the proposed threshold is exceeded.

In Case 3, f_2 occurs due to a mass increase of 26 kg and occurs after 10 s ($t_f = 10$). In Fig. 12, it can be also seen that, with the nominal control, we have the maximum permissible error of 2°, When we add the FTC, the fault effect is compensated. In Fig. 13, fault detection occurs when the proposed threshold is exceeded.

Note 3. It is important to detect the fault, otherwise only by compensating its effect, and not repairing, there may be a breakdown or a catastrophe observed.

With the simulation results it was observed that the objective is to maintain the trajectory within an interval; while it is maintained within this zone, we can say that the fault is being tolerated.

5. Conclusion

This paper proposed an efficient FTC scheme for trajectory tracking in Euler–Lagrange systems, which increases the fault size that can be tolerated by a close-loop system.

A supplementary control action is added in order to compensate the fault effect when it is present in the system. One outstanding feature of the proposed scheme is that it integrates the benefits of robust GPI observer-based control to estimate the faults and to perform the compensation.

The proposed scheme performs better than a simple GPI observer-based control when used as a nominal control. The advantages of the proposed approach are that it uses an additional control loop, which allows keeping the nominal control law unchanged, and does not require information from the entire mathematical model (it only requires the inertial matrix). The simulation results confirm satisfactory closed-loop performance in terms of trajectory tracking and fault tolerance. Some disadvantages could be the requirement of richness in frequency components of the signals involved in the GPI observer, and that the proposed approach does not distinguish between perturbation and faults.

In our future work we will consider the possibility of reducing model dependency for fault compensation.

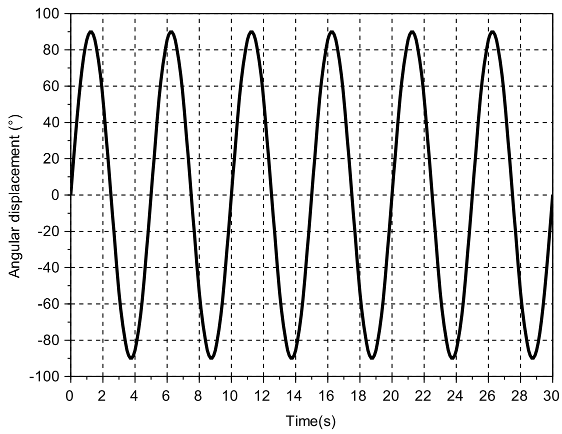

Fig. 8. Nominal trajectory (y_n).

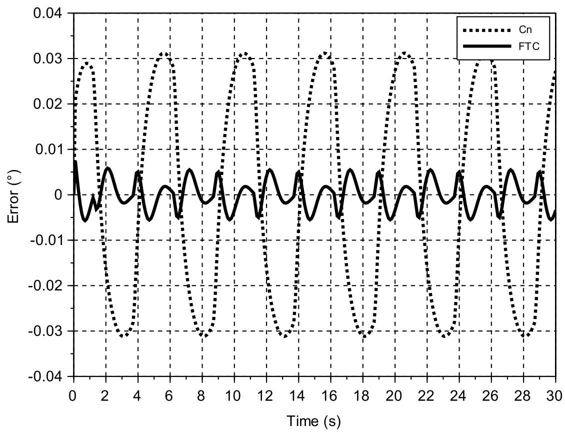

Fig. 9. Tracking error (nominal conditions).

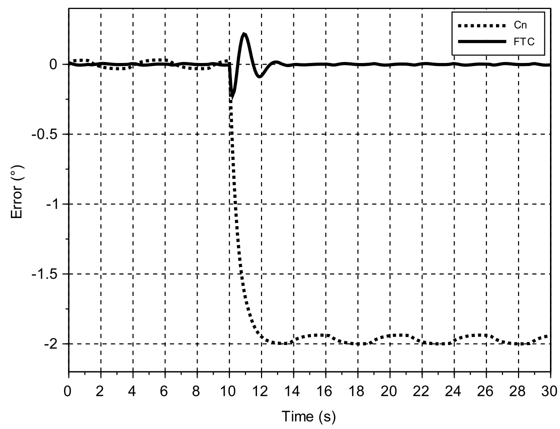

Fig. 10. Tracking error in the presence of f_1.

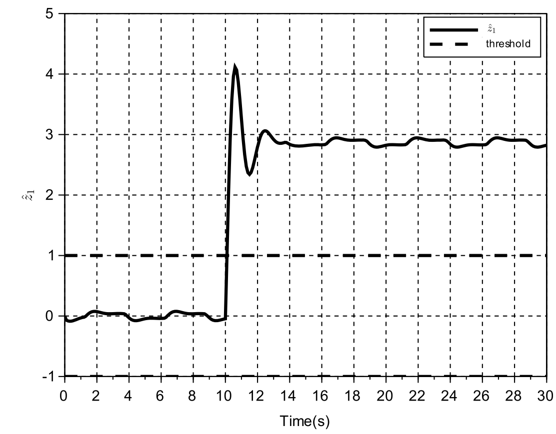

Fig. 11. Uncertain polynomial (f_1).

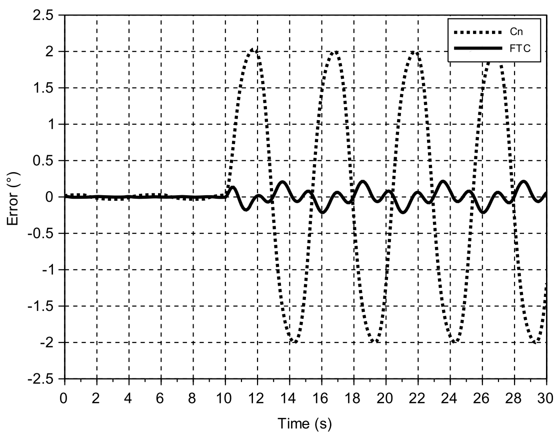

Fig. 12. Tracking error in the presence of f_2.

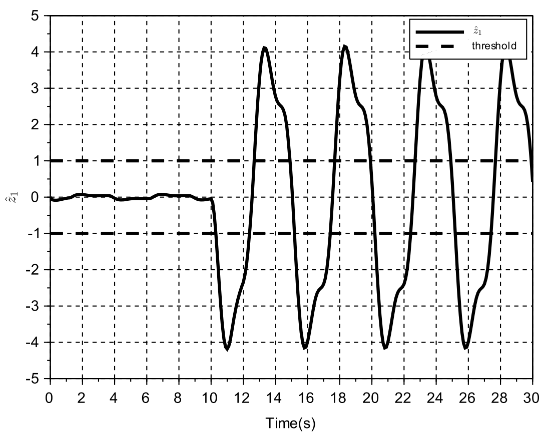

Fig. 13. Uncertain polynomial (f_2).

Acknowledgment

The authors would like to thank CONACyT-Mexico for the support.

References

Acosta-Santana, P., Rodriguez-Alfaro, L. and Alcorta-Garcia, E. (2013). A cascade structure approach to control reconfiguration, *Conference on Control and Fault-Tolerant Systems (SysTol), Nice, France*, pp. 347–352.

Blanke, M., Kinnaert, M., Lunze, J., Staroswiecki, M. and Schröder, J. (2016). *Diagnosis and Fault-Tolerant Control*, Springer, Berlin/Heidelberg.

Bolton, W. (2021). *Instrumentation and Control Systems*, 3rd Edn, Newnes, Oxford.

Cieslak, J., Henry, D. and Zolghadri, A. (2010). Fault tolerant flight control: From theory to piloted flight simulator experiments, *IET Control Theory & Applications* **4**(8): 1451–1464.

Cieslak, J., Henry, D., Zolghadri, A. and Goupil, P. (2008). Development of an active fault-tolerant flight control strategy, *Journal of Guidance, Control, and Dynamics* **31**(1): 135–147.

Flores-Flores, J.P. and Martinez-Guerra, R. (2019). PI observer design for a class of nondifferentially flat systems, *International Journal of Applied Mathematics and Computer Science* **29**(4): 655–665, DOI: 10.2478/amcs-2019-0048.

Gao, Z., Cecati, C. and Ding, S.X. (2015). A survey of fault diagnosis and fault-tolerant techniques. Part I: Fault diagnosis with model-based and signal-based approaches, *IEEE Transactions on Industrial Electronics* **62**(6): 3757–3767, DOI: 10.1109/TIE.2015.2417501.

Gutiérrez Giles, A., Arteaga Pérez, M.A. and Sira Ramírez, H. (2016). Force control of robot manipulators based on generalized proportional integral observers, *Ibero-American Journal of Automation and Industrial Computing* **13**(2): 238–246.

Hamayun, M.T., Edwards, C., Alwi, H. and Bajodah, A. (2015). A fault tolerant direct control allocation scheme with integral sliding modes, *International Journal of Applied Mathematics and Computer Science* **25**(1): 93–102, DOI: 10.1515/amcs-2015-0007.

Kailath, T. (1980). *Linear Systems*, Prentice-Hall, Englewood Cliffs.

Kelly, R. and Santibáñez, V. (2003). *Control de movimiento de robots manipuladores*, Pearson, Madrid.

Krokavec, D., Filasová, A. and Liščinskỳ, P. (2016). LMI-based design of cascade reconfiguration control structures, *3rd Conference on Control and Fault-Tolerant Systems (SysTol), Barcelona, Spain*, pp. 605–610.

Li, S., Wang, H., Aitouche, A., Tian, Y. and Christov, N. (2018). Active fault tolerance control of a wind turbine system using an unknown input observer with an actuator fault, *International Journal of Applied Mathematics and Computer Science* **28**(1): 69–81, DOI: 10.2478/amcs-2018-0005.

Ortega, R., Perez, J.A.L., Nicklasson, P.J. and Sira-Ramirez, H.J. (2013). *Passivity-based Control of Euler–Lagrange Systems: Mechanical, Electrical and Electromechanical Applications*, Springer, London.

Rodriguez-Alfaro, L., Alcorta-Garcia, E. and Espinosa-Pérez, G. (2013). A cascade approach for fault-tolerant active control in MSIP, *National Congress of Automatic Control 2013, Ensenada, Baja California, Mexico*, pp. 245–250.

Salazar, J.C., Sanjuan Gómez, A., Nejjari Akhi-Elarab, F. and Sarrate Estruch, R. (2020). Health-aware and fault-tolerant control of an octorotor UAV system based on actuator reliability, *International Journal of Applied Mathematics and Computer Science* **30**(1): 47–59, DOI: 10.34768/amcs-2020-0004.

Sira-Ramírez, H., Luviano-Juárez, A., Ramírez-Neria, M. and Zurita-Bustamante, E.W. (2018). *Active Disturbance Rejection Control of Dynamic Systems: A Flatness Based Approach*, Butterworth-Heinemann, Oxford.

Sira-Ramírez, H., Ramírez-Neria, M. and Rodríguez-Angeles, A. (2010). On the linear control of nonlinear mechanical systems, *49th IEEE Conference on Decision and Control (CDC), Atlanta, USA*, pp. 1999–2004.

Van der Schaft, A.J. (2000). *L_2-Gain and Passivity Techniques in Nonlinear Control*, Vol. 2, Springer, London.

Yu, X. and Jiang, J. (2015). A survey of fault-tolerant controllers based on safety-related issues, *Annual Reviews in Control* **39**: 46–57.

Ivon E. Leal-Leal was born in Monterrey, Nuevo Leon, Mexico, in 1992. She received her BSc degree in electronics and automation engineering and her MSc in electrical engineering from Universidad Autónoma de Nuevo Leon (UANL), Mexico, in 2013 and 2016, respectively, where she is currently pursuing her PhD degree in electrical engineering. Her present research interests include automation control, fault diagnosis and fault tolerant control.

Efrain Alcorta-Garcia was born in Monterrey, Nuevo Leon, Mexico, in 1968. He received his BSc degree in electronics and communications engineering and his MSc degree in electrical engineering (automatic control) from Universidad Autónoma de Nuevo León (UANL), Mexico, in 1989 and 1992, respectively, and his PhD degree in electrical engineering (automatic control) from the Gerhard Mercator University of Duisburg, Germany, in 1999. Since 1999 he has held a teaching and research position at UANL. His research interests include model-based fault diagnosis, fault tolerant control and observers.

Received: 11 April 2022
Revised: 14 August 2022
Accepted: 18 September 2022